

# Bulk electronic structure of optimally doped $\text{Ba}(\text{Fe}_{1-x}\text{Co}_x)_2\text{As}_2$

C. Utfeld,<sup>1</sup> J. Laverock,<sup>1</sup> T. D. Haynes,<sup>1</sup> S. B. Dugdale,<sup>1</sup> J. A. Duffy,<sup>2</sup> M. W. Butchers,<sup>2</sup> J. W. Taylor,<sup>3</sup> S. R. Giblin,<sup>3</sup> J. G. Analytis,<sup>4,5</sup> J. Chu,<sup>4,5</sup> I. R. Fisher,<sup>4,5</sup> M. Itou,<sup>6</sup> and Y. Sakurai<sup>6</sup>

<sup>1</sup>*H. H. Wills Physics Laboratory, University of Bristol,  
Tyndall Avenue, Bristol BS8 1TL, United Kingdom*

<sup>2</sup>*Department of Physics, University of Warwick, Coventry CV4 7AL, United Kingdom*

<sup>3</sup>*ISIS Facility, Rutherford Appleton Laboratory, Chilton, Oxfordshire OX11 0QX, United Kingdom*

<sup>4</sup>*Stanford Institute for Materials and Energy Sciences,*

*SLAC National Accelerator Laboratory, 2575 Sand Hill Road, Menlo Park, CA 94025*

<sup>5</sup>*Geballe Laboratory for Advanced Materials and Department of Applied Physics, Stanford University, CA 94305*

<sup>6</sup>*Japan Synchrotron Radiation Research Institute,  
SPring-8, 1-1-1 Kouto, Sayo, Hyogo 679-5198, Japan*

(Dated: May 20, 2022)

We report high-resolution, bulk Compton scattering measurements unveiling the Fermi surface of an optimally-doped iron-arsenide superconductor,  $\text{Ba}(\text{Fe}_{0.93}\text{Co}_{0.07})_2\text{As}_2$ . Our measurements are in agreement with first-principles calculations of the electronic structure, revealing both the  $X$ -centered electron pockets and the  $\Gamma$ -centered hole pockets. Moreover, our data are consistent with the strong three-dimensionality of one of these sheets that has been predicted by electronic structure calculations. Complementary calculations of the non-interacting susceptibility,  $\chi_0(\mathbf{q}, \omega)$ , suggest that the broad peak that develops due to interband Fermi surface nesting, and which has motivated several theories of superconductivity in this class of material, survives the three-dimensional Fermi surface topology of this family.

PACS numbers: 71.18.+y, 74.70.-b, 78.70.Ck

The discovery of superconductivity in  $\text{LaO}_{1-x}\text{F}_x\text{FeAs}$ , a member of the so-called ‘1111’ family of iron-pnictide materials [1], has triggered intense research into its nature and origin. Tempted by the proximity of the superconductivity in these compounds to an antiferromagnetic spin density wave (SDW) state, many theoretical models have focused on spin fluctuations as the key [2, 3], supported by first-principles calculations of the electronic structure. Such calculations predict four Fermi surface (FS) sheets: two hole sheets at the center of the Brillouin zone (BZ), and two electron sheets centered at its corner [4, 5]. In the undoped (and lightly doped) ‘1111’ compounds the hole and electron sheets are well nested, leading to a broad peak in the non-interacting susceptibility [2]. The spin fluctuations that are thought to develop from this FS instability have already been observed in neutron scattering measurements [6], and theoretical models suggest they promote a strongly pairing interaction, provided that the order parameter changes phase between the hole and electron FS sheets (the so-called  $s_{\pm}$ -model) [2, 3]. Central to such models, however, is a detailed understanding of the topology of the FS; here we present a bulk measurement of the FS of an optimally-doped iron-arsenide superconductor,  $\text{Ba}(\text{Fe}_{0.93}\text{Co}_{0.07})_2\text{As}_2$ , alongside complementary calculations of the non-interacting susceptibility,  $\chi_0(\mathbf{q}, \omega)$ .

$\text{Ba}(\text{Fe}_{1-x}\text{Co}_x)_2\text{As}_2$  is a member of the ‘122’ family of iron-pnictide superconductors, with a maximum  $T_c \sim 24\text{ K}$  for  $x \sim 0.06$  [7, 8]. Unlike the ‘1111’ family, whose FS is quasi-2D, the ‘122’ compounds are predicted by electronic structure calculations to have substantial 3D

warping of one of the hole sheets [5], the degree of which is sensitive to the position of the As with respect to the Fe plane. Nonetheless, both families exhibit nesting between parallel pieces of the hole and electron FS sheets. Neutron scattering measurements reveal spin fluctuations at the FS nesting vector, which is coincident with the AFM wavevector for both ‘1111’ and ‘122’ compounds [6]. For  $\text{Fe}(\text{Te}, \text{Se})$ , where the nesting vector is not coincident with the AFM wavevector, spin fluctuations are only evident at the FS nesting vector [9], indicating that the long-range magnetic order is not FS driven [10].

Experimentally, de Haas-van Alphen (dHvA) measurements have found good agreement with local density approximation (LDA) calculations, observing orbits that correspond to both electron and hole FS sheets in  $\text{LaFePO}$  [11] and non-superconducting  $\text{SrFe}_2\text{P}_2$  [12]. Indeed, only small rigid shifts of the LDA band structure were required in both cases to achieve good agreement with the experimental data. However, owing to restrictions imposed by the electron mean free path, these measurements have so far been confined to the stoichiometric compounds, away from the maximum  $T_c$ . Angle-resolved photoemission (ARPES) measurements, on the other hand, yield a more contradictory picture. Whereas some measurements on the undoped or lightly-doped  $\text{BaFe}_2\text{As}_2$  system demonstrate reasonable broad, albeit qualitative, agreement with LDA predictions [13, 14, 15], others suggest either the existence of hole-like ‘blades’ in place of the quasi-2D electron sheets expected at the corner of the BZ [16] that are interpreted as indicative of additional order, or do not simultaneously observe

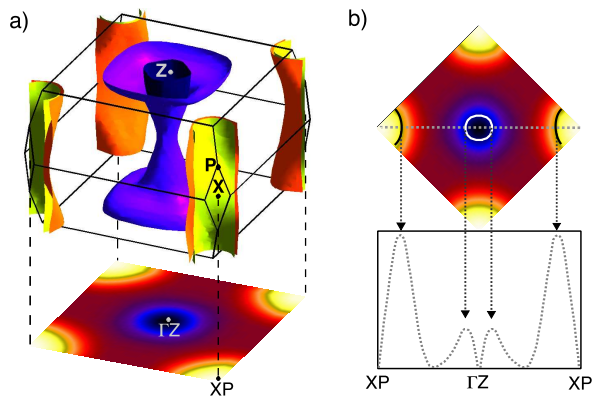


FIG. 1: (Color online) (a) The LDA FS of  $\text{Ba}(\text{Fe}_{0.93}\text{Co}_{0.07})_2\text{As}_2$  (top), and its relation to the occupation density projected down the  $c^*$ -axis (bottom). Note that the occupation density has been convoluted with the experimental resolution function. (b) The overlaid FS contours (black and white lines, top) are identified via the maxima in (the absolute value of) the first derivative of the occupation density shown at the bottom along a projected, high symmetry path.

both hole and electron FS sheets. Indeed, scanning-tunneling microscopy has been applied to the surface layers of  $\text{Ba}(\text{Fe}_{0.93}\text{Co}_{0.07})_2\text{As}_2$ , finding a complex array of sample-dependent (specifically, cleavage temperature) ordered and disordered structures [17], which are not representative of the bulk electronic structure.

More recently, several ARPES studies [13, 18, 19], supported by dHvA [12] measurements, have reported on the 3D nature of the ‘122’ family FS, and particularly the warping of one of the hole FS sheets that has been predicted by electronic structure calculations [5]. The FS that has motivated spin-fluctuation models of superconductivity has so far been quite 2D, employing either the quasi-2D band structure of  $\text{LaFeAsO}_{1-x}\text{F}_x$  [2] or a 2D minimal model of it [3]. Since the warping is expected to extend over some quarter of the  $c^*$ -axis, the question of whether the nesting instabilities that are expected to drive the spin fluctuations are robust against such three dimensionality must be raised.

Compton scattering provides a valuable complement to dHvA and ARPES, unambiguously probing the occupied states of the *bulk* electronic structure. Its insensitivity to defects or disorder make it an ideal technique for tackling the FS of disordered systems (e.g. [20]) and, since it is sensitive to the bulk 3D momentum density, it is able to provide information about the FS throughout the BZ. In this study the occupation density, featuring the projected Fermi breaks, serves as the key quantity for assessing the FS of  $\text{Ba}(\text{Fe}_{0.93}\text{Co}_{0.07})_2\text{As}_2$ .

A Compton profile represents a double integral (1D projection) of the underlying 3D electron momentum density (EMD), in which the FS manifests itself via discontinuous breaks. Six Compton profiles equally spaced

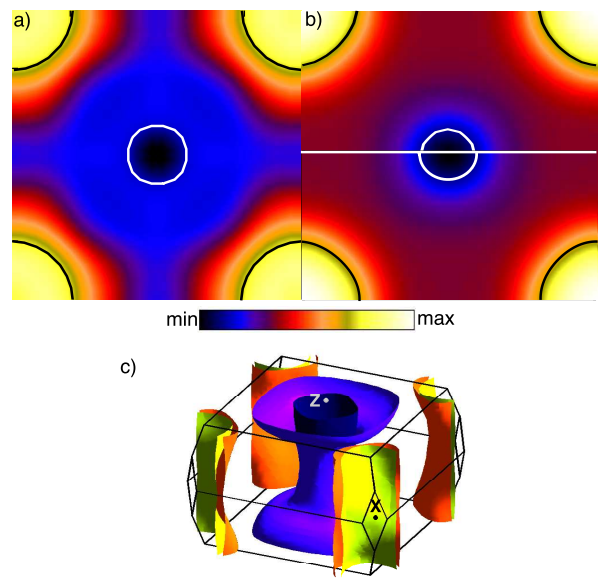


FIG. 2: (Color online) The occupation density of  $\text{Ba}(\text{Fe}_{0.93}\text{Co}_{0.07})_2\text{As}_2$  from (a) experimental Compton scattering measurements at 295 K and (b) the electronic structure calculations of Fig. 1a from the original calculation (top), and after rigidly shifting the bands (see text, bottom). In (c) the FS corresponding to the shifted bands is shown for comparison with Fig. 1a.

between [100] and [110] were measured at room temperature ( $T = 295\text{ K}$ ) on the high-resolution Compton spectrometer of beamline BL08W at the SPring-8 synchrotron [21]. This spectrometer consists of a Cauchois-type crystal analyzer and a position-sensitive detector, with a resolution FWHM at the Compton peak of 0.105 a.u. (1 a.u. of momentum =  $1.99 \times 10^{-24}\text{ kg m s}^{-1}$ ). For each Compton profile,  $\sim 480\,000$  counts were accumulated in the peak data channel, and each Compton profile was corrected for possible multiple-scattering contributions using a Monte Carlo method [22]. Details of the sample growth and characterization may be found in Ref. [8].

For the purpose of comparison with the occupation density predicted by band theory and to aid interpretation of our data, we performed *ab initio* calculations of the electronic structure of  $\text{Ba}(\text{Fe}_{0.93}\text{Co}_{0.07})_2\text{As}_2$  using the full-potential linearized augmented plane wave method [23] within the LDA, where the effect of doping was included via the virtual crystal approximation (VCA) [25]. Fig. 1a shows the calculated FS, composed of two quasi-2D electron sheets and two hole sheets, in agreement with previous calculations for similar Co concentrations [5, 26]. Note the considerable three-dimensionality (‘warping’) of the outer hole sheet.

Using tomographic techniques [27], it is possible to reconstruct the 2D (or, if a sufficiently large number of profiles can be measured, even 3D e.g. [20]) EMD from a specially chosen set of 1D Compton profiles. Here, our

six Compton profiles were reconstructed to obtain the 2D EMD projected along the  $c^*$ -axis, which was then folded back into the first BZ using the Lock-Crisp-West (LCW) procedure [28]. This culminates in a projected occupation density, shown for the data in Fig. 2a, representing a projection of the occupied electron states in the BZ, where light (dark) colors represent high (low) occupation densities. As can be seen from the data, both the electron and hole FS sheets that are predicted by electronic structure calculations (Fig. 2b) are clearly identifiable, with the electron sheets in the corner of the projected BZ ( $XP$ ) and the hole sheets in the center,  $\Gamma Z$ . It is worth emphasizing that although this quantity is 2D, information on the third, projected dimension is still stored in the integral. For an ideally 2D FS, the Fermi breaks would be realised as a step function between high and low occupation densities broadened only by the experimental resolution; however, the three-dimensionality of the FS results in an additional smearing of these projected breaks.

In order to refine this picture, a method for detecting the FS breaks via the first derivative of the occupation density, as illustrated in Fig. 1b for the theoretical result, was employed. The subtraction of an isotropic component, corresponding to the more isotropic, tightly-bound electron states, from the data before applying the LCW procedure yields further enhancement in locating the Fermi breaks and hence the maxima in the first derivative of this quantity were used to locate the breaks, and the occupation density as contoured at the corresponding level [29]. Fig. 2a shows overlaid on the data the experimental Fermi surface breaks mapped out utilizing this method. Owing to the experimental resolution and the projected nature of this result, two features should be noted: Firstly, the two electron (hole) sheets are not resolved individually and secondly, the contours here represent an average over the shape and size of the FS sheets projected down the  $c^*$ -axis. The slightly larger size of the electron compared with the hole pockets is expected as a consequence of electron doping. For these (experimental) contours assuming a quasi-2D FS topology, this leads to an occupied volume of the BZ of  $4.38 \pm 0.16$  electrons. In comparison, for  $\text{Ba}(\text{Fe}_{0.93}\text{Co}_{0.07})_2\text{As}_2$ , the FS should enclose 4.14 electrons, and we now focus on an explanation for the discrepancy between these two figures.

In Fig. 2b, the same procedure that was applied to the data has been employed for the theoretical FS, which explicitly includes the three-dimensionality of the outer hole sheet, and good agreement is found between experiment and theory. However, our method for locating the Fermi breaks relies on a peak in the first derivative of the occupation density, and as demonstrated in Fig. 1b, no such peak is discernible in the theoretical occupation density that corresponds to the wider part of the ‘warped’ hole FS. In projection, and with our experimental resolution, this feature is not resolvable and is therefore

expected to be absent in the experimental contours as well. On the other hand, since some of the hole FS is not accounted for in the contours, the ‘warping’ still leaves its mark in the occupation density in the form of an imbalance in the detected electron count. Indeed, we find that 4.34 electrons are enclosed by our theoretical contours, where the excess electrons stem from an *underestimation* of the volume of the hole FS, i.e. as a direct consequence of the ‘warping’ of one of those cylinders. Since the theoretical 3D FS used in this analysis unambiguously encloses 4.14 electrons, this supports well the notion that the extra electrons in our experimental contours provide strong evidence of the 3D warping of the hole FS. It should be noted that the theoretical FS is calculated with the As atoms at the LDA minimum [5]; our calculations at the experimental As position, in which the ‘warping’ is much weaker, were not able to explain such a mismatch in the occupied fraction of the BZ.

Turning our attention to the details of the FS contours, and their comparison with theory, our data suggest slightly larger FS sheets than those expected from the calculation. It is instructive to investigate whether such a discrepancy can be accounted for by a rigid shift of the theoretical band energies, in such a way that the electron sheets increase in size while the overall electron count in the system is maintained by a shift on the hole sheets. As can be seen in Fig. 2b, shifts of  $\sim -120$  meV and  $\sim +80$  meV for the electron and hole bands respectively leads to a good overall agreement between data and theory, in which the shifted theoretical contours now enclose 4.40 electrons. As illustrated in Fig. 2c employing such shifts preserves the FS topology, only affecting the size of the hole and electron pockets.

Overall, the projected FS topology obtained in our study is in good agreement with other measurements on similar compounds (e.g. [12, 13, 15]), as well as electronic structure calculations within the LDA. In Ref. [12], a rigid shift of the theoretical electronic structure was required to well-reproduce their quantum oscillations measurements on  $\text{SrFe}_2\text{P}_2$ . Those shifts were of a similar magnitude, and were in the opposite direction; however, the necessary additional approximations employed in this calculation (for example, the VCA, which describes the disorder and is an average potential approximation) may play a role here. Additionally, our data show no evidence of the propeller-like structure near the  $X$ -point that has recently been reported in some ARPES measurements [16].

The nesting between these hole and electron FS sheets has been implicated in several models of superconductivity, motivated by a quasi-2D FS topology that provides ample nesting throughout the  $c^*$ -axis of the BZ [2, 3], as evidenced by the broad peak in the susceptibility near  $\mathbf{q} = (\pi, \pi)$  [2]. However, for the ‘112’ compounds presented here, our data, in agreement with some ARPES and dHvA studies [12, 13, 18, 19], suggest that an appre-

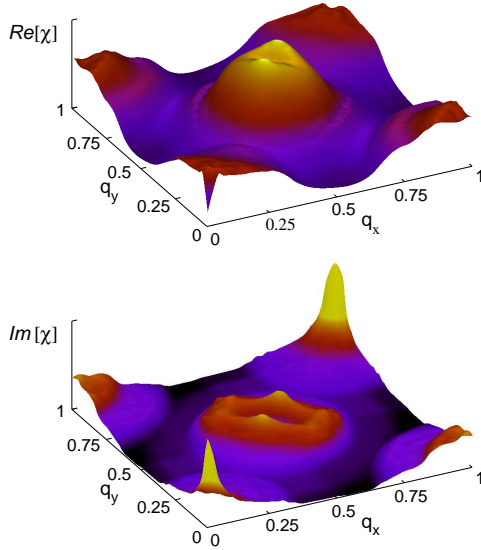


FIG. 3: (Color online) The (a) real and (b) imaginary parts of the static susceptibility,  $\chi(\mathbf{q}, 0)$ , of  $\text{Ba}(\text{Fe}_{0.93}\text{Co}_{0.07})_2\text{As}_2$ .

cial portion of the FS along the  $c^*$ -axis does not nest at the same wavevector. In order to address what impact this may have on the susceptibility of the system, we have calculated the non-interacting susceptibility,  $\chi_0(\mathbf{q}, \omega)$ , for wavevector  $\mathbf{q}$  and frequency  $\omega$  [2]. Both real and imaginary parts of  $\chi_0(\mathbf{q}, \omega)$  were calculated for the (raw, unshifted) electronic structure of  $\text{Ba}(\text{Fe}_{0.93}\text{Co}_{0.07})_2\text{As}_2$ , and are shown in Fig. 3. Despite the three-dimensionality of the FS, a substantial (although broad) peak in the imaginary part of  $\chi_0(\mathbf{q})$ , whose origin lies in FS nesting, survives into the real part, with a maximum at  $\mathbf{q}_{\text{max}} \approx (0.56, 0.56)\pi/a$ . This broadly peaked structure bears close resemblance to that calculated for the ‘1111’ compounds in Ref. [2], although the strength of the peak is slightly weaker here due to the ‘warping’ in  $k_z$ . The wavevector of the maximum itself,  $\mathbf{q}_{\text{max}}$  agrees favorably with the nesting vector obtained from our experimental contours of  $\mathbf{q}_{\text{exp}} \approx (0.62, 0.62)\pi/a$ , given that our contours represent an *average* of the FS sheets (applying the same procedure to the convoluted theoretical occupation density yields  $\mathbf{q}_{\text{the}} \approx (0.61, 0.61)\pi/a$ ). That our experimental results are in good agreement with the LDA calculation, particularly with the topology of the FS, provides experimental evidence that the  $s_{\pm}$ -model may still provide a route to superconductivity in the ‘122’ compounds, despite the enhanced three-dimensionality of the electronic structure.

In conclusion, the FS topology of  $\text{Ba}(\text{Fe}_{0.93}\text{Co}_{0.07})_2\text{As}_2$  has been investigated using Compton scattering, a true bulk probe of the occupied electron states. Good agreement is found between our experimental projected FS and the predictions of the LDA, which can be max-

imised by employing only small, rigid shifts of the theoretical electronic structure. In particular, our data cannot be explained without including the strong three-dimensionality of the hole FS expected for the ‘122’ family. However, our calculations of the non-interacting susceptibility of this compound suggest that the peak that has been implicated in some theories of superconductivity survives this three-dimensionality, and may still be available as a mechanism in these compounds.

### Acknowledgments

We would like to thank C. Lester and S.M. Hayden for their technical assistance. We acknowledge the financial support from the UK EPSRC. This experiment was performed with the approval of the Japan Synchrotron Radiation Research Institute (JASRI, proposal no. 2009A1094). Work at Stanford University is supported by the Department of Energy, Office of Basic Energy Sciences under contract DE-AC02-76SF00515.

- 
- [1] Y. Kamihara *et al.*, J. Am. Chem. Soc. **130**, 3296 (2008).
  - [2] I.I. Mazin, D.J. Singh, M.D. Johannes and M.-H. Du, Phys. Rev. Lett. **101**, 057003 (2008).
  - [3] K. Kuroki *et al.*, Phys. Rev. Lett. **101**, 087004 (2008).
  - [4] D.J. Singh and M.-H. Du, Phys. Rev. Lett. **100**, 237003 (2008).
  - [5] D.J. Singh, Phys. Rev. B **78**, 094511 (2008).
  - [6] A.D. Christianson *et al.*, Nature (London) **456**, 930 (2009); J. Zhao *et al.*, arXiv:0908.0954v1 (2009); M.D. Lumsden *et al.*, Phys. Rev. Lett. **102**, 107005 (2009); J. Zhao *et al.*, Nature Phys. (preprint) (2009).
  - [7] N. Ni *et al.*, Phys. Rev. B **78**, 214515 (2008).
  - [8] J.-H. Chu, J.G. Analytis, C. Kucharczyk and I.R. Fisher, Phys. Rev. B **79**, 014506 (2009).
  - [9] Y. Qiu *et al.*, Phys. Rev. Lett. **103**, 067008 (2009). H.A. Mook *et al.*, arXiv:0904.2178 (2009).
  - [10] M.D. Johannes and I.I. Mazin, Phys. Rev. B **79**, 220510(R) (2009).
  - [11] A.I. Coldea *et al.*, Phys. Rev. Lett. **101**, 216402 (2008).
  - [12] J.G. Analytis *et al.*, Phys. Rev. Lett. **103**, 076401 (2009).
  - [13] W. Malaeb *et al.*, arXiv:0906.1846v1 (2009).
  - [14] V. Brouet *et al.*, arXiv:0907.5379v1 (2009); H. Ding *et al.*, Europhys. Lett. **83**, 47001 (2008).
  - [15] M. Yi *et al.*, Phys. Rev. B **80**, 024515 (2009);
  - [16] V.B. Zabolotnyy *et al.*, Nature (London) **457**, 569 (2009).
  - [17] F. Massee *et al.*, arXiv:0907.5544v1 (2009).
  - [18] P. Vilmercati *et al.*, Phys. Rev. B **79**, 220503(R) (2009).
  - [19] C. Liu *et al.*, Phys. Rev. Lett. **102**, 167004 (2009).
  - [20] S.B. Dugdale *et al.*, Phys. Rev. Lett. **96**, 046406 (2006).
  - [21] N. Hiraoka *et al.*, J. Synchrotron Radiat. **8**, 26 (2004); Y. Sakurai and M. Itou, J. Phys. Chem. Solids **65**, 2061 (2004).
  - [22] N. Sakai, J. Phys. Soc. Jpn. **56**, 2477 (1987).
  - [23] P. Blaha *et al.*, WIEN2k, an Augmented Plane Wave + Local Orbitals Program for Calculating Crystal Proper-

- ties* (K. Schwarz, Technical University of Wien, Vienna, Austria, 2002), ISBN 3-9501031-1-2.
- [24] M. Rotter *et al.*, Phys. Rev. B **78**, 020503(R) (2008).
  - [25] Convergence was achieved over 635  $k$ -points in the irreducible BZ. The structural parameters were those of Ref. [24], with the exception that the position of the As atom was at the LDA minimum by Ref. [5].
  - [26] A.S. Sefat *et al.*, Phys. Rev. Lett. **101**, 117004 (2008).
  - [27] G. Kontrym-Sznajd, Phys. Status Solidi A **117**, 227 (1990).
  - [28] D.G. Lock, V.H.C. Crisp and R.N. West, J. Phys. F: Metal Physics **3**, 561 (1973).
  - [29] Applying the same procedure to our calculations was found to yield a relative enhancement of the projected Fermi breaks, without influencing the location at which they were identified.